Geomechanics and Engineering, *Vol. 13, No. 3 (2017) 517-533*
DOI: https://doi.org/10.12989/gae.2017.13.3.517

Stability analysis of homogeneous slopes with benches

Lianheng Zhao [**1,2], Peng Xia [1], Rongfu Xie [3],
Liang Li [1], Yingbin Zhang [*4,5] and Xiao Cheng [1]

[1] *School of Civil Engineering, Central South University, Changsha, Hunan 410075, China*
[2] *Key Laboratory of Heavy-Haul Railway Engineering Structure, Ministry of Education, Central South University, Changsha, Hunan 410075, China*
[3] *Xiamen Municipal Engineering Design Institute Co., Ltd., Xiamen, Fujian 361004, China*
[4] *Key Laboratory of Transportation Tunnel Engineering, Ministry of Education, Southwest Jiaotong University, Chengdu 610031, China*
[5] *Department of Geotechnical Engineering, School of Civil Engineering, Southwest Jiaotong University, Chengdu 610031, China*

(*Received November 26, 2015, Revised April 07, 2017, Accepted April 26, 2017*)

Abstract. In this paper, with a graphical approach, a series of stability charts for homogeneous slopes with benches are presented based on the upper bound limit analysis theory and strength reduction technique. The objective function of the slope safety factor F_s is optimized by the nonlinear sequential quadratic programming, and a substantial number of examples are illustrated to use the stability charts for homogeneous slopes with benches driven by only the action of the soil weight. These charts can be applied to quick and accurate estimations of the stability status of homogeneous slopes with benches. Moreover, the failure modes and the formula for safety factor Fs of homogeneous slopes with benches are provided to illustrate the stability analysis of slopes with benches, which is validated by samples.

Keywords: slope stability analysis; safety factor; shear strength reduction technique; limit analysis

1. Introduction

Stability charts have been studied by many researchers to quickly estimate the stability of a slope. Taylor (1937) developed stability charts used in the stability analysis for clay slopes, based on the friction circle method in which the algorithm needs iteration. Bishop and Morgenstern (1960), Bell (1966), Cousins (1978), Michalowski (Michalowski 2002, 2010, Michalowski and Martel 2011), Steward *et al*. (2011) and Eid (2014) improved the Taylor charts by eliminating the iterative steps in the calculation of safety factor F_s. Klar *et al*. (2011) proposed new stability charts for simple earth slopes without iteration, based on the limit equilibrium method as well as its relationship with the probability of slope instability. Sun and Zhao (2013) developed previous research and drew up stability charts considering pore water pressure to quickly calculate the safety factor F_s and determine the types of slope failure. Tang *et al*. (2015) put forward stability

∗Corresponding author, Ph.D., Associate Professor, E-mail: yingbinz516@126.com
** Co-corresponding author, Ph.D., Professor, E-mail: zhaolianheng@csu.edu.cn

http://www.techno-press.org/?journal=gae&subpage=7 ISSN: 2005-307X (Print), 2092-6219 (Online)

charts under typical environment loads, with which the safety factor F_s and the failure mode can be determined quickly.

All the charts mentioned above aim at simple slopes and focus less on slopes with benches normally used in engineering practice. Using the upper bound limit analysis, Gao *et al*. (2013, 2014) derived formulae for overall instability and possible local instability appearing in slopes with benches, and discussed the influence of heterogeneity and anisotropic nature of the cohesive force on slope stability. Pantelidis and Psaltou (2012) used the software SLIDE^{TM} for numerous calculations and gave a series of stability tables for calculating the stability factor as well as for judging the local instability of slopes with benches under conditions such as those prevailing in some typical slope geometry and groundwater. Because of the nature of the iterative process for calculating the stability factor, these stability tables could not give rapid assessment of the typical slopes with benches used in engineering practice for calculating the safety factor F_s.

This paper aims at presenting a series of stability charts for slopes with benches, based on the graphical approach proposed by Klar *et al*. (2011). This paper also extends the work of Pantelidis and Psaltou (2012) by presenting stability charts of slope with beaches. Compared with the previous methods, one of the advantages of the present method is the slope safety factor can been obtained indirectly without iterative calculation. The logarithmic spiral rotational failure mode for homogeneous slopes with benches is adopted based on the upper bound limit analysis (Chen 1975, Dawson *et al*. 1999, Baker 2006, Zhao *et al*. 2010, 2015, 2016). By using the shear strength reduction technique, this paper derives the formula for the safety factor F_s of homogeneous slopes with benches. It also gives stability charts for homogeneous slopes with benches, which can help us to perform rapid assessment of the safety factor of homogeneous slopes with benches driven by only the action of the soil weight. The results are expected to provide reasonable references for the primary design of slopes with benches in engineering and for rapid evaluation of slope stability.

2. Stability analysis for slopes with benches

In this paper, the slope stability analysis of homogeneous slopes with benches is conducted based on the upper bound limit analysis and shear strength reduction technique. The strength reduction technique is widely used in the analysis of stability safety factor F_s, based on the linear Mohr-Coulomb (M-C) failure criterion (Zienkiewicz *et al*. 1975, Duncan 1996, Griffiths and Lane 1999 and Steward *et al*. 2011). It is assumed that the shear strength of the geo-material is factored by the safety factor F_s, and when the slope reaches the critical state, the slope failure occurs exactly. At this state, the sliding mass performs rigid rotation around the center of rotation and the geo-materials of the slope conform to the associated flow rule. The safety factor F_s above is generally defined as follows

$$F_s = \frac{c}{c_m} = \frac{\tan\varphi}{\tan\varphi_m} \tag{1}$$

where c and φ are the original shear strength parameters, and c_m and φ_m are the reduced ones.

2.1 Failure mode of slopes with benches

The experimental results of a large number of scaled models for homogeneous and isotropic slopes show that failure surfaces of homogeneous slopes are closer to logarithmic spiral sliding

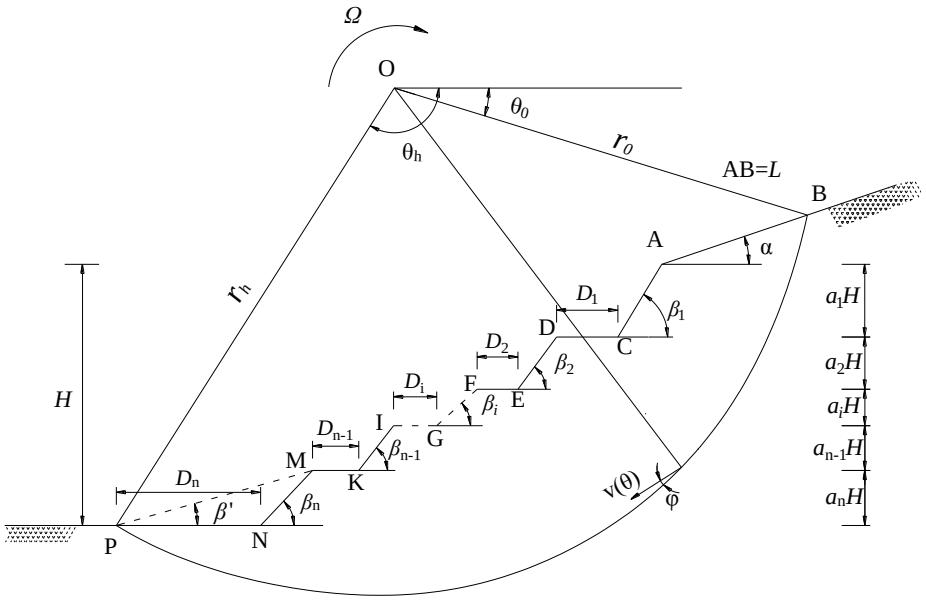

Fig. 1 Logarithmic spiral sliding plane for slopes with benches

surface, as shown in Fig. 1. The rigid body *BPNMKIGFEDCA* performs rigid rotation around the center *O*, and under the logarithmic spiral surface *BC*', which is a thin layer whose thickness can be ignored, the soil body is stationary. There are *n*-1 benches on the slope and their widths (D_1 – $D_{n\text{-}1}$) are marked in Fig. 1 in the order from top to bottom. There are *n*-4 benches omitted between the bench *EF* and *KM*, whose widths are D_i. In particular, D_n is the distance from slope toe *N* to point *P* which can be determined after optimization of the failure surface *BP*.

2.2 Overall stability analysis for slopes with benches

According to the upper bound limit analysis, the rate of work created by slope external loading is made equal to the internal energy dissipation rate of the rock and soil mass on the basis of the principle of minimum stream power, and the energy dissipation equilibrium equation is established. The rate of internal energy dissipation refers to the energy dissipation occurring at the logarithmic spiral intersection surface. The external power in this paper refers only to the one created by sliding mass weight.

In the rotational failure analysis for a slope with benches, the factored shear strength parameters can be introduced into the external forces work equation and the internal energy dissipation equation.

According to the principle of analysis of energy consumption, the rate of work created by external loading is made equal to the internal energy dissipation rate for a slope with factored shear strength parameters c_m and φ_m, and then an expression of upper bound safety factor F_s of slopes with benches can be given

$$F_s = \frac{c}{\gamma H} \frac{e^{2\left[(\theta_h-\theta_0)\tan\varphi_m\right]}-1}{2\tan\varphi_m\left(f_1' - f_2' - \cdots - f_{2n+1}' - f_{2n+2}'\right)}\left(\frac{H}{r_0}\right) \tag{2}$$

where H is the critical height of slope; γ is the unit weight of geo-materials; H/r_0 and functions f_1 to f_{2n+2} are functions of θ_h, θ_0, α, β_0……β_n, α_0……α_n, β' and φ, whose expressions are given in the Appendix I. The difference between functions f'_1 to f'_{2n+2} and functions f_1 to f_{2n+2} is that in functions f_1 to f_{2n+2} φ is replaced by φ_m = arctan (tan φ/F_s).

2.3 Local stability analysis for slopes with benches

Sometimes overall instability does not always appear in steep slopes with benches, while local instability occurs instead because only a part of the sub-slope reaches the limit state.

It is compared with the safety factor F_s of overall instability that the local stability can be calculated by referring to formula (2), with the corresponding adjustment of geometrical parameters. Taking an example of a slope with three benches, which is typical in engineering practice, the possible local failure modes are shown in Fig. 2, as well as the latent sliding plane. The critical latent slip surface is determined as the one with the smallest safety factor F_s by random searching and analyzing multiple possible sliding surfaces.

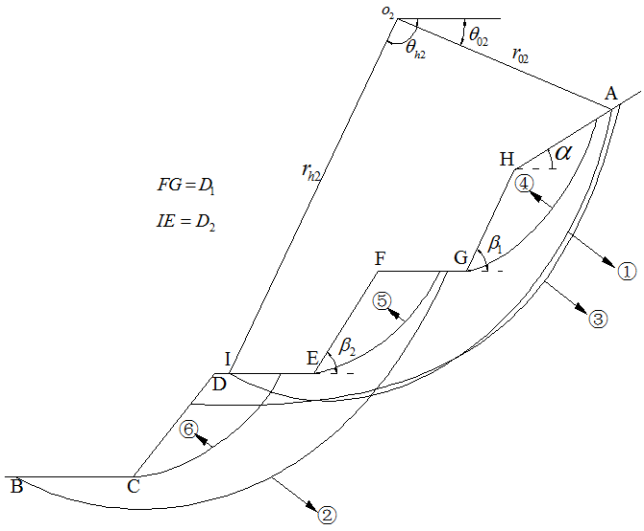

Fig. 2 Possible local failure modes for slopes with three benches (Gao *et al.* 2014)

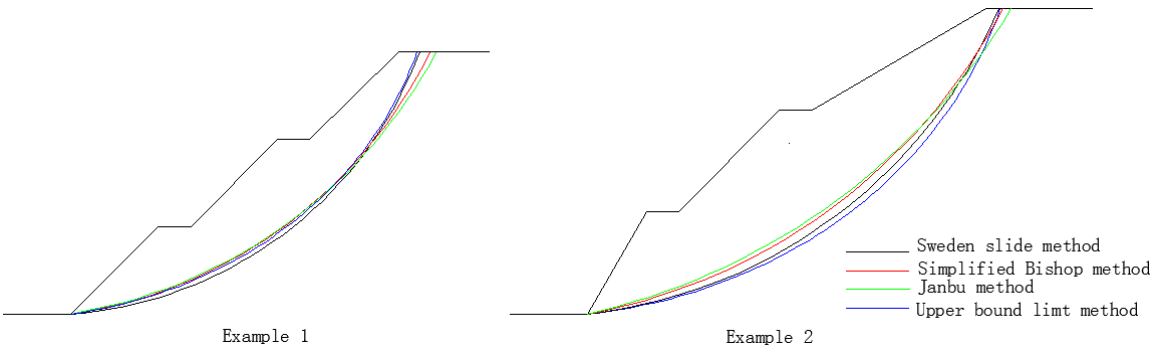

Fig. 3 Comparison of sliding surfaces for overall instability in examples

Table 1 Comparison for safety factor F_s with overall instability in slopes with three benches

Examples	c /kPa	φ /°	γ /kN·m^{-3}	α_1	α_2	α_3	β_1 /°	β_2 /°	β_3 /°	H /m	D /m	Safety factor F_s			
												Sweden Slide method	Simplified Bishop method	Janbu method	This paper
1	28	25	18.5	1/3	1/3	1/3	45	45	45	24	3	1.282	1.343	1.353	1.217
2	30	20	17.85	2/7	3/7	2/7	30	45	60	28	3	1.068	1.099	1.105	1.028

Table 2 Comparison of safety factors F_s for local instability

Method	Failure mode	Example		
		1	2	3
This paper	Local instability of two benches	1.266	1.465	
	Local instability of single bench			1.268
Simplified Bishop method	Local instability of two benches	1.358	1.506	
	Local instability of single bench			1.298
Janbu method	Local instability of two benches	1.378	1.516	
	Local instability of single bench			1.330

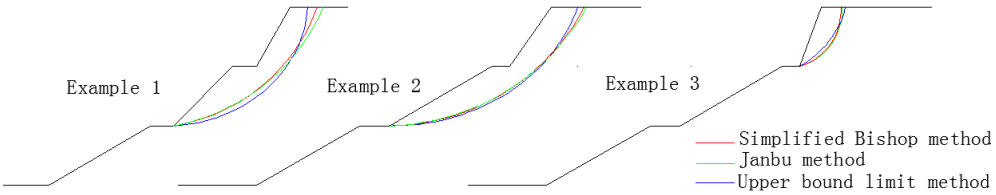

Fig. 4 Comparison of sliding surfaces for local instability

* Example 1: The height of the slope with three benches (H) is 30 m. The depth coefficient for each bench ($a_1 = a_2 = a_3$) is 1/3. The angle of the toe of the benches is $\beta_1 = 60°$, $\beta_2 = 45°$, and $\beta_3 = 30°$. The angle of the top of the slope (α) is 0°. The width of the benches is $D_1 = D_2 = 4$ m. The parameters of the soil body are $\gamma = 18.5$ kN/m^3, $c = 30$ kPa, and $\varphi = 25°$.
* Example 2: $H = 30$ m. $a_1 = a_2 = a_3 = 1/3$, $\beta_1 = 55°$, $\beta_2 = \beta_3 = 30°$, $\alpha = 0°$, $D_1 = 2$ m, $D_2 = 4$ m, $\gamma = 20$ kN/m^3, $c = 20$ kPa, and $\varphi = 30°$.
* Example 3: $H = 30$ m, $a_1 = a_2 = a_3 = 1/3$, $\beta_1 = 70°$, $\beta_2 = \beta_3 = 30°$, $\alpha = 0°$, $D_1 = 3$ m, $D_2 = 5$ m, $\gamma = 17.8$ kN/m^3, $c = 25$ kPa, and $\varphi = 38°$.

2.4 Nonlinear programming method

In Eq. (2), β_0……β_n, α_0……α_n, γ and H are known parameters, and the strength reduction indexes (c_m, φ_m) are related to the original shear strength parameters (c and φ). The strength reduction technique can be expressed as that: Given known slope conditions (β_0……β_n, α_0……α_n, γ, H), the slope is at a limit equilibrium status when the shear strength indexes (c and φ) are reduced to a condition (c_m, φ_m) such that the critical height is equal to the actual original height ($H = H_{cr}$). Then, the safety factor F_s can be found by solving the following equations

$$\min \quad F_s = F_s\left(\theta_0,\ \theta_h,\ \beta'\right) \tag{3}$$

$$\text{s.t.} \quad \begin{cases} 0<\beta' \le \pi \\ 0<\theta_0<\pi/2 \\ \theta_0<\theta_h<\pi \end{cases} \tag{4}$$

In Eq. (2), the unknown variable are θ_h, θ_0, β' and $\boldsymbol{F}_s$. The solution of Eq. (2) can be obtained through optimization, which yields both the $\boldsymbol{F}_s$ values and the position of the potential sliding surface. An optimization procedure utilizing a sequential quadratic programming algorithm is used to obtain the minimum $\boldsymbol{F}_s$ in this paper (Tang *et al*. 2015). The slope stability analysis program which is based on the upper bound theorem of limit analysis has been developed by applying a nonlinear sequential quadratic programming algorithm and using the method of exhaustion to avoid sticking at local optima.

2.5 Comparison and analysis

To prove the correctness of formulas derived in this paper, slopes with three benches are considered as examples to analyze the slopes for overall and local stability, which are typical in engineering practice.

2.5.1 Overall stability analysis

Results comparison of examples with that of existing methods are shown in Table 1 and Fig. 3. It reveals that the slope safety factor F_s based on both upper bound limit analysis and shear strength reduction technique is slightly smaller than those based on other methods, thus it proves the accuracy and validity of the method adopted in this paper.

2.5.2 Local stability analysis

The literature (Gao *et al*. 2014) reveals that two main types of local instability are possible for slopes with three benches, including local instability for two benches (as sliding surfaces ①② shown in Fig. 2) and local instability for single bench (as sliding ④⑤⑥ surfaces shown in Fig. 2). The results of local stability analysis of three slope examples with benches are shown in Table 2 and Fig. 4.

The results show that the slope safety factor obtained by the methods adopted by this paper is slightly smaller than those obtained by the other two methods, indicating that the formula proposed in this paper is accurate and valid.

3. Graphical approach for homogeneous slopes

3.1 Dimensionless parameters

Stability charts for homogeneous slopes can be used to quickly analyze slope safety factor F_s. In order to simplify this type of charts, Taylor (1948), Das and Sobhan (2013), Klar *et al*. (2011), Sun and Zhao (2013), and Duncan and Wright (1980) introduced three dimensionless parameters: $\lambda_{c\varphi}$, $\tan\varphi$ and N. The value of $\lambda_{c\varphi}$ controls the location of the potential sliding surface of homogeneous slopes which means slopes with the same value of $\lambda_{c\varphi}$ have the same critical slip

surface. A higher value of $\lambda_{c\varphi}$ means that the critical slip surface is nearer to the slope surface. A slope with a certain combination of N, $\tan\varphi$ and β has the only safety factor F_s (Jiang and Yamagami 2006, 2008).

$$N = \frac{c}{\gamma H} \tag{5}$$

$$\lambda_{c\varphi} = \frac{\gamma H \tan\varphi_f}{c_f} = \frac{\gamma H(\tan\varphi / F_s)}{c / F_s} = \frac{\gamma H \tan\varphi}{c} \tag{6}$$

3.2 Graphical approach for safety factor F_s

Klar *et al*. (2011) and Sun and Zhao (2013) put forward a graphical approach based on the limit equilibrium method to quickly determine the safety factor F_s of homogeneous slope (as shown in Fig. 5). The curve g shows the relationship between $\tan\varphi$ and $c/\gamma H$ when the slope is at a state of limit equilibrium. A homogeneous slope with a ($c/\gamma H$, $\tan\varphi$) combination positioned on curve g is at a state of critical instability, while a combination positioned above the curve g is stable. The gradient of line OA is equal to $\lambda_{c\varphi}$, and the slopes with the ($c/\gamma H$, $\tan\varphi$) combination on the same line OA refer to the same slope failure surface (Jiang and Yamagami 2006, 2008). According to the geometric relation between the curve g and line OA, Klar *et al*. (2011) and Sun and Zhao (2013) proposed a method for rapid calculation of slope safety factor F_s

$$F_s = \frac{a}{b} = \frac{x_1}{x_2} = \frac{y_1}{y_2} \tag{7}$$

In the above formula, a is the length of line OA, b is the distance between origin and (x_2, y_2). x_1, y_1, x_2, and y_2 are abscissas and ordinates of point A and the intersection point of OA and curve g, respectively. The value of F_s determined by formula (7) equals the value of F_s determined by the shear strength reduction technique in formula (1).

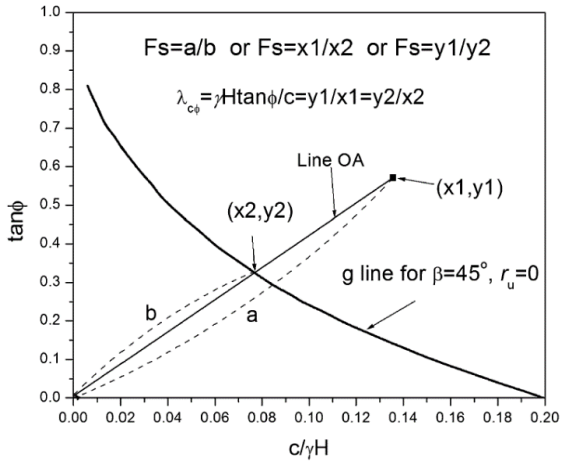

Fig. 5 Graphic approach to determining homogeneous simple slope safety factor F_s (Klar *et al*. 2011, Sun and Zhao 2013)

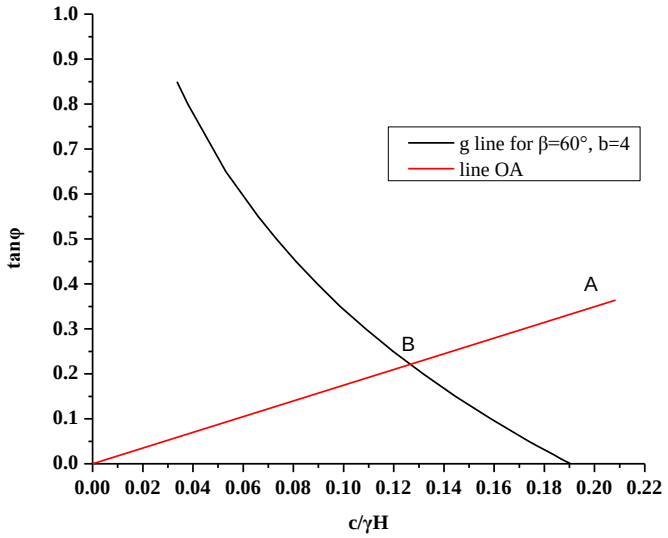

Fig. 6 Stability chart for homogeneous slopes with two benches

3.3 Stability analysis with graphical approach for homogeneous slopes with benches

Referring to the study of Klar *et al*. (2011) and Sun and Zhao (2013), there is a simple deduction for slopes with regular geometric surface which are typical in engineering practice, that the location of the sliding surface under the condition of overall instability relates only to the dimensionless parameter $\lambda_{c\varphi}$, and there exists the same relationship, i.e., curve *g*, between another dimensionless parameter $c/\gamma H$ and tanφ. Once curve *g* and line OA for slopes with benches are drawn up, the safety factor F_s can be calculated quickly according to formula (5).

Suppose there is a soil slope with two benches (H = 12 m, $a_1 = a_2$ = 0.5, $\beta_1 = \beta_2$ = 60°, α = 0°, D = 4 m, γ = 20 kN/m^3, c = 50 kPa, and φ = 20°). According to the upper bound theorem of limit analysis, the slope safety factor F_s is calculated by the method of sequential quadratic programming, and the result is F_s = 1.6460.

The corresponding curve *g* and line OA are then drawn. The coordinates of A and B are (0.2083, 0.3640) and (0.1266, 0.2213), respectively. According to formula (5), the slope safety factor F_s is 0.2083/0.1266 = 1.6453 and F_s = 0.3640/0.2213 = 1.6448, which are similar.

4. Stability charts for homogeneous slopes with benches

4.1 Stability charts for simple slopes

The objective function of the safety factor F_s of a homogeneous slope with benches is optimized by the nonlinear sequential quadratic programming.

The stability charts (as shown in Fig. A1 in Appendix II) are drawn for simple homogeneous slopes (the angles are 30°, 45°, 60°, 75° and 90°).

To calculate the safety factor F_s of a certain slope, both curve *g* and line OA are necessary. Curve *g* can be chosen only by angle β, and line OA can be determined according to the physical

parameters of the soil and the total height of the slope. Thus, slope stability can be quickly assessed with the charts given in this paper.

4.2 Stability charts for homogeneous slopes with benches

Design charts are presented below for homogeneous slopes with benches commonly used in practice, for the slope angles of 30°, 45°, 60° and 75°; The width of the bench is 2 m, 3 m, or 4 m. The safety factor F_s for homogeneous bench slopes with other parameters can be calculated simply by interpolation.

To develop stability charts for homogeneous slopes with two to five benches, a large number of cases were analyzed using the nonlinear programming. Only considering the normal condition for homogeneous slopes with two to five benches under self-weight, the stability charts regardless of the exterior conditions were obtained as shown in Figs. A2-A5 in Appendix II. It should be noted that $H = 2.5\ h$ means $a_1/a_3 = 0.5$ and $a_2 = a_3$, and $H = 3h$ means $a_1 = a_2 = a_3$ in Fig. A3; $H = 3.5\ h$ means $a_1/a_4 = 0.5$ and $a_2 = a_3 = a_4$, and $H = 4h$ means $a_1 = a_2 = a_3 = a_4$ in Fig. A4; $H = 4.5\ h$ means $a_1/a_5 = 0.5$ and $a_2 = a_3 = a_4 = a_5$, and $H = 5\ h$ means $a_1 = a_2 = a_3 = a_4 = a_5$ in Fig. A5.

It can be observed from Figs. A2 to A5 in Appendix II that curve g is steeper when the slope angle β increases. When the other parameters of multi-stage slopes under simple conditions (e.g., the mechanical parameters c, γ, and φ and geometric parameters β_i and H) are determined, the width of the bench D and the depth coefficient α_i make little difference to the slope safety factor F_s.

For the stability assessment of a certain homogeneous slope with benches, charts should be applied appropriately according to the geometry of a slope, especially the depth coefficients and the width of the benches. To simplify the description of slope geometry, a slope with a depth coefficient of $a_1/a_2 = 0.5$ is presented as the ratio of the total height H to the height of the last stage h ($H = 1.5\ h$), while $H = 3\ h$ means $a_1 = a_2 = a_3$. The same method is applied to the rest of the cases. This paper presents stability charts for homogeneous slopes with bench widths of 2 m, 3 m, and 4 m and different angles (30°, 45°, 60°, 75° and 90°). The charts have $c/\gamma H$ and $\tan\varphi$ on the axes, avoiding the influence of single parameters such as slope total height H, cohesion c, and unit weight of soil γ.

5. Examples

5.1 Case 1 ($H = 4\ h$, $D = 4\ m$)

A homogeneous slope with four benches of height 28 m and constant toe angle 45° is used to illustrate the application of stability charts presented with depth coefficients of $a_1 = a_2 = a_3 = a_4$ ($H = 4\ h$) and bench width of 4 m. The physical parameters of the soil are $\gamma = 20$ kN/m^3, $c = 50$ kPa and $\varphi = 28°$. Hence, $c/\gamma H = 50/(20\times28) = 0.09$ and $\tan\varphi = 0.53$.

It can be determined from Fig. A4(f)) in Appendix II that x for the intersection point is 0.06 (0.0617), and the safety factor F_s can thus be computed by formula (5) for $F_s = 0.09/0.06 = 1.50$. It can be seen that the safety factor F_s presented in the stability chart is slightly less than the value 1.56 calculated using programming, which verifies the validity of the charts.

5.2 Case 2 ($H = 1.8\ h$, $D = 3\ m$)

A homogeneous slope with two benches having height 18 m, depth coefficient of $a_1/a_2 = 0.8$, constant toe angle 30° and bench width of 3 m is used to examine the application of stability charts.

The following soil characteristics were considered: γ = 17.8 kN/m^3, c = 20 kPa and φ = 15°. Based on the above data, $c/\gamma H$ = 0.06 and tanφ = 0.27 can be obtained.

The ordinates of the intersection point can be found equal to 0.24 (0.2406) and 0.24 (0.2419) from Fig. A2(b) and (e) respectively in Appendix II. Accordingly, both of the safety factors F_s are calculated as 1.13 by formula (5). So the charts are valid because the safety factor F_s obtained in this paper is slightly less than that of 1.14 calculated by programming.

5.3 Case 3 ($H = 3\ h$, $D = 2.5$ m)

Consider a homogeneous slope with three benches as an example, with height 18 m ($a_1 = a_2 = a_3$), constant toe angle 60°, bench width 2.5 m and three soil parameters: γ = 15 kN/m^3, c = 35 kPa and φ = 25°. Hence, the values of $c/\gamma H$ and tanφ are computed as 0.13 and 0.47, respectively.

The y-coordinates of the intersection can be determined as 0.35 (0.3547) and 0.35 (0.3534) from Fig. A3(d) and (e) respectively in Appendix II. The safety factors F_s are the same value 1.34, which can be computed by formula (5). The charts in this paper can obtain less safety factor F_s than the programming (1.37), proving that the charts is accurate again.

5.4 Case 4 ($H = 2.7\ h$, $D = 3.3$ m)

To further demonstrate the application of stability charts, another homogeneous slope with three benches is adopted, which is characterized by height 27 m (with depth coefficients of a_1/a_2 = 0.7 and $a_2 = a_3$), constant toe angle 45° and bench width 3.3 m, and whose physical parameters are γ = 18.5 kN/m^3, c = 40 kPa and φ = 25°. Therefore, the dimensionless parameters $c/\gamma H$ = 0.08 and tanφ = 0.47 are computed.

It can be found from Figs. A3(b) and (c) in Appendix II that the vertical ordinates for the intersection point is 0.36 (0.3646) and 0.34 (0.3449), respectively. The safety factors F_s can thus be computed by formula (5) for 1.31 and 1.38. Therefore, the safety factor F_s for the case of (H = 2.5 h, D = 3.3 m) can be obtained as 1.33 through interpolation calculation. At the same time, the safety factor F_s for the case of (H = 3 h, D =3.3 m) can be calculated from Figs. A3(e) and (f) in Appendix II as 1.33. Thus, the safety factor F_s for the case of (H = 2.7 h, D = 3.3 m) can be obtained as 1.33 by interpolation calculation and is slightly less than the value 1.34 calculated using nonlinear programming, verifying the validity of the charts.

6. Conclusions

The objective function of the safety factor F_s of the overall stability for homogeneous slopes with benches was implemented.

- This paper gives stability charts on the basis of the shear strength reduction technique under simple condition where the safety factors F_s of homogeneous slopes with benches can be quickly calculated. It can be used in engineering practice for the primary design, checking the software results, and quick stability assessment of slopes with benches.
- On the one hand, when other parameters of slopes with benches under simple conditions are determined, the width of the bench D and the depth coefficient α_i make little difference to the slope safety factors F_s. On the other hand, increasing the number of slope benches and reducing the depth coefficient are useful for reducing the lateral pressure of the slopes and

construction difficulty and enhancing the slope stability. This is of great importance in the case of slopes with high fill and deep excavation.

The slope stability analysis in this paper, which was based on homogeneous slopes with benches, can be further developed to obtain stability charts under other environmental loads, such as the surcharge load, seismic load and pour water pressure. There is scope to further discuss and improve the application of stability charts for slopes with benches in engineering practice.

Acknowledgments

The research described in this paper was financially supported by the Natural Science Foundation of China (No. 51408511, 51478477 and 41672286), Innovation-Driven Project of Central South University (No. 2016CX012) and the Guizhou Provincial Department of Transportation Foundation (No. 2012122033, 2014122006). All financial supports are greatly appreciated.

References

Baker, R. (2006), "A relation between safety factors with respect to strength and height of slopes", *Comput. Geotech.*, **33**(4), 275-277. DOI: 10.1016/j.compgeo.2006.07.001

Bell, J.M. (1966), "Dimensionless parameters for homogeneous earth slopes", *Soil Mech. Found. Div., Am. Soc. Civ. Eng.*, **92**(5), 51-65. DOI: 10.1016/0022-4898(67)90127-9

Bishop, A.W. and Morgenstern, N.R. (1960), "Stability coefficients for earth slopes", *Geotechnique*, **10**(4), 129-150. DOI: 10.1680/geot.1960.10.4.129

Chen, W.F. (1975), *Limit Analysis and Soil Plasticity*, Elsevier Scientific Publishing Company, New York, NY, USA.

Cousins, B.F. (1978), "Stability charts for simple earth slopes", *J. Geotech. Eng. Div., Am. Soc. Civ. Eng.*, **104**(2), 267-279. DOI: 10.1016/0148-9062(78)91396-7

Das, B. and Sobhan, K. (2013), *Principles of Geotechnical Engineering*, Cengage Learning.

Dawson, E.M., Roth, W.H. and Drescher, A. (1999), "Slope stability analysis by strength reduction", *Géotechnique*, **49**(6), 835-840.

Duncan, J.M. and Wright, S.G. (1980), "The accuracy of equilibrium methods of slope stability analysis", *Eng. Geol.*, **16**(1), 5-17. DOI: 10.1016/0013-7952(80)90003-4

Duncan, J.M. (1996), "State of the art: Limit equilibrium and finite-element analysis of slopes", *Geotech. Eng. ASCE*, **122**(7), 577-596. DOI: 10.1061/(ASCE)0733-9410(1996)122:7(577)

Eid, H.T. (2014), "Stability charts for uniform slopes in soils with nonlinear failure envelopes", *Eng. Geol.*, **168**, 38-45. DOI: 10.1016/j.enggeo.2013.10.021

Gao, L.S., Zhao, L.H. and Tang, G.P. (2013), "Upper bound limit analysis of stability on inhomogeneity and anisotropy two-stage slope", *Electro. J. Geotech. Eng.*, **18**(Q), 3581-3604.

Gao, L.S., Yi, D. and Mao, N. (2014), "Upper bound limit analysis of stability on multi-level slope with benches", *J. Highway Transport. Res. Develop.*, **6**(31), 1-10.

Griffiths, D.V. and Lane, P.A. (1999), "Slope stability analysis by finite elements", *Géotechnique*, **49**(3), 387-403.

Jiang, J.C. and Yamagami, T. (2006), "Charts for estimating strength parameters from slips in homogeneous slopes", *Comput. Geotech.*, **33**(6), 294-304. DOI: 10.1016/j.compgeo.2006.07.005

Jiang, J.C. and Yamagami, T. (2008), "A new back analysis of strength parameters from single slips", *Comput. Geotech.*, **35**(2), 286-291. DOI: 10.1016/j.compgeo.2007.09.004

Klar, A., Aharonov, E., Kalderon-Asael, B. and Katz, O. (2011), "Analytical and observational relations

between landslide volume and surface area", *J. Geophys. Res.: Earth Surf.* (2003-2012), **116**(F2). DOI: 10.1029/2009JF001604

Michalowski, R.L. (2002), "Stability charts for uniform slopes", *J. Geotech. Geoenviron.Eng.*, **128**(4), 351-355. DOI: 10.1061/(ASCE)1090-0241(2002)128:4(351)

Michalowski, R.L. (2010), "Limit analysis and stability charts for 3D slope failures", *J. Geotech. Geoenviron. Eng.*, **136**(4), 583-593. DOI: 10.1061/(ASCE)GT.1943-5606.0000251

Michalowski, R.L. and Martel, T. (2011), "Stability charts for 3D failures of steep slopes subjected to seismic excitation", *J. Geotech. Geoenviron. Eng.*, **137**(2), 183-189. DOI: 10.1061/(ASCE)GT.1943-5606.0000412

Pantelidis, L. and Psaltou, E. (2012), "Stability tables for homogeneous earth slopes with benches", *Int. J. Geotech. Eng.*, **6**(3), 381-394. DOI: 10.3328/IJGE.2012.06.03.381-394

Steward, T., Sivakugan, N., Shukla, S.K. and Das, B.M. (2011), "Taylor's slope stability charts revisited", *Int. J. Geomech.*, **11**(4), 348-352. DOI: 10.1061/(ASCE)GM.1943-5622.0000093

Sun, J.P. and Zhao, Z. (2013), "Stability charts for homogenous soil slopes", *J. Geotech. Geoenviron. Eng.*, **139**(12), 2212-2218. DOI: 10.1061/(ASCE)GT.1943-5606.0000938

Tang, G.P., Zhao, L.H., Li, L. and Yang, F. (2015), "Stability charts of slopes under typical conditions developed by upper bound limit analysis", *Comput. Geotech.*, **65**, 233-240. DOI: 10.1016/j.compgeo.2014.12.008

Taylor, D.W. (1937), "Stability of earth slopes", *Boston Soc. Civil Eng.*, **24**(3), 197-247.

Taylor, D.W. (1948), *Fundamentals of Soil Mechanics*, John Wiley & Sons, New York, NY, USA.

Zhao, L.H., Li, L., Yang, F., Luo, Q. and Liu, X. (2010), "Upper bound analysis of slope stability with nonlinear failure criterion based on strength reduction technique", *J. Central South Univ. Technol.*, **17**(4), 836-844. DOI: 10.1007/s11771-010-564-7

Zhao, L., Yang, F., Zhang, Y., Dan, H. and Liu, W. (2015), "Effects of shear strength reduction strategies on safety factor of homogeneous slope based on a general nonlinear failure criterion", *Comput. Geotech.*, **63**, 215-228. DOI: 10.1016/j.compgeo.2014.08.015

Zhao, L.H., Cheng, X., Zhang, Y., Li, L. and Li, D.J. (2016), "Stability analysis of seismic slopes with cracks", *Comput. Geotech.*, **77**, 77-90. DOI: 10.1016/j.compgeo.2016.04.007

Zienkiewicz, O.C., Humpheson, C. and Lewis, R.W. (1975), "Associated and nonassociated viscoplasticity in soil mechanics", *Géotechnique*, **25**(4), 671-689.

CC

Appendix I

$$\frac{H}{r_0}=\frac{\sin\left(\theta_h+\alpha\right)e^{(\theta_h-\theta_0)\tan\varphi}-\sin\left(\theta_0+\alpha\right)+\sin\alpha\cdot\sum_{i=1}^{n-1}\frac{D_i}{r_0}}{\cos\alpha-\sin\alpha\cdot\left(\sum_{i=1}^{n-1}\alpha_i\cot\beta_i+\alpha_n\cot\beta'\right)} \tag{A1}$$

$$\frac{L}{r_0}=\frac{1}{\sin\alpha}\left\{\sin\theta_h\cdot e^{(\theta_h-\theta_0)\tan\varphi}-\sin\theta_0-\frac{H}{r_0}\right\} \tag{A2}$$

$$\frac{D_n}{r_0}=\alpha_n\cdot\left(\cot\beta'-\cot\beta_n\right)\cdot\frac{H}{r_0} \tag{A3}$$

$$f_1=\frac{\left\{\left(\sin\theta_h+3\tan\varphi\cos\theta_h\right)\cdot e^{\left[3\cdot(\theta_h-\theta_0)\cdot\tan\varphi\right]}-\left(3\cdot\tan\varphi\cdot\cos\theta_0+\sin\theta_0\right)\right\}}{3\left(1+9\cdot\tan^2\varphi\right)} \tag{A4}$$

$$f_2=\frac{1}{6}\frac{L}{r_0}\cdot\sin\left(\alpha+\theta_0\right)\cdot\left(2\cos\theta_0-\frac{L}{r_0}\cos\alpha\right) \tag{A5}$$

$$f_3=\frac{\alpha_1}{6}\left(\frac{H}{r_0}\right)\begin{bmatrix}\cos\theta_0-\left(\cos\alpha\right)\left(\dfrac{L}{r_0}\right)+\\ \sin\theta_0\cot\beta_1+\cot\beta_1\left(\dfrac{L}{r_0}\right)\sin\alpha\end{bmatrix}\cdot\left[2\cos\theta_0-2\cos\alpha\left(\frac{L}{r_0}\right)-\alpha_1\cot\beta_1\left(\frac{H}{r_0}\right)\right] \tag{A6}$$

$$f_4=\frac{1}{6}\left(\frac{D_1}{r_0}\right)\left[\sin\theta_0+\frac{L}{r_0}\sin\alpha+\alpha_1\left(\frac{H}{r_0}\right)\right]\begin{bmatrix}2\cos\theta_0-2\cos\alpha\left(\dfrac{L}{r_0}\right)\\ -2\alpha_1\cot\beta_1\left(\dfrac{H}{r_0}\right)-\dfrac{D_1}{r_0}\end{bmatrix} \tag{A7}$$

when $3\le i\le n$

$$\begin{aligned}f_{2i-1}=\frac{\alpha_{i-1}}{6}\cdot\frac{H}{r_0}\cdot\Bigg\{&\Bigg[\cos\theta_0-\cos\alpha\cdot\frac{L}{r_0}-\frac{H}{r_0}\cdot\sum_{j=1}^{i-2}\alpha_j\cot\beta_j-\sum_{j=1}^{i-2}\frac{D_j}{r_0}\cdot\\ &+\left(\sin\theta_0+\sin\alpha\cdot\frac{L}{r_0}\right)\cdot\cot\beta_{i-1}+\frac{H}{r_0}\cdot\cot\beta_{i-1}\cdot\sum_{j=1}^{i-2}\alpha_j\Bigg]\\ &\cdot\left[2\cos\theta_0-2\cos\alpha\cdot\frac{L}{r_0}-2\frac{H}{r_0}\cdot\sum_{j=1}^{i-2}\alpha_j\cot\beta_j-2\cdot\sum_{j=1}^{i-2}\frac{D_j}{r_0}-\alpha_{i-1}\cot\beta_{i-1}\cdot\frac{H}{r_0}\right]\Bigg\}\end{aligned} \tag{A8}$$

$$f_{2i}=\frac{1}{6}\cdot\frac{D_{i-1}}{r_0}\cdot\left\{\begin{array}{l}\left(\sin\theta_0+\dfrac{L}{r_0}\sin\alpha+\dfrac{H}{r_0}\cdot\sum\limits_{j=1}^{i-1}\alpha_j\right)\cdot\\ \left(2\cos\theta_0-2\dfrac{L}{r_0}\cos\alpha-2\dfrac{H}{r_0}\cdot\sum\limits_{j=1}^{i-1}\alpha_j\cot\beta_j-2\cdot\sum\limits_{j=1}^{i-2}\dfrac{D_j}{r_0}-\dfrac{D_{i-1}}{r_0}\right)\end{array}\right\} \tag{A9}$$

$$f_{2n+1}=\frac{\alpha_n}{6}\cdot\frac{H}{r_0}\cdot\frac{\sin(\theta_h+\beta')}{\sin\beta'}\cdot\mathrm{e}^{(\theta_h-\theta_0)\tan\varphi}\cdot\left[2\cos\theta_h\,\mathrm{e}^{(\theta_h-\theta_0)\tan\varphi}+\alpha_n\frac{H}{r_0}\cot\beta'\right] \tag{A10}$$

$$f_{2n+2}=\frac{\alpha_n}{6}\cdot\frac{D_n}{r_0}\cdot\frac{H}{r_0}\cdot\left[3\cos\theta_h\,\mathrm{e}^{(\theta_h-\theta_0)\tan\varphi}+\frac{D_n}{r_0}+\alpha_n\frac{H}{r_0}\cot\beta'\right] \tag{A11}$$

Appendix II

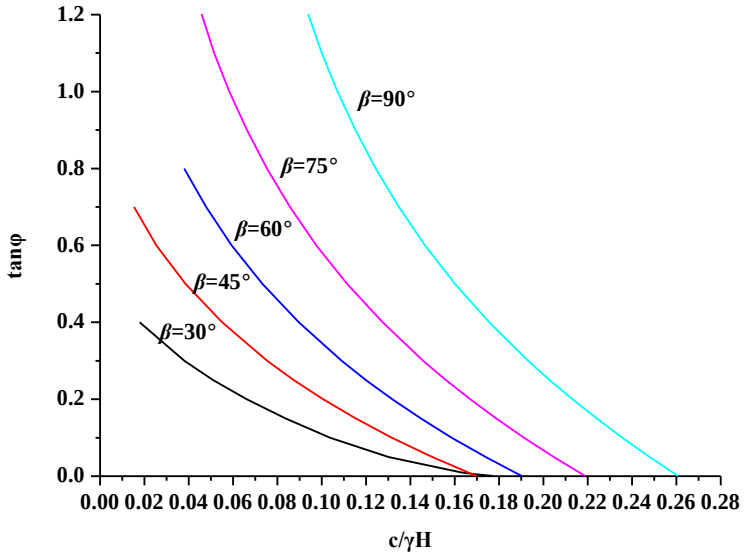

Fig. A1 Stability charts for simple slopes

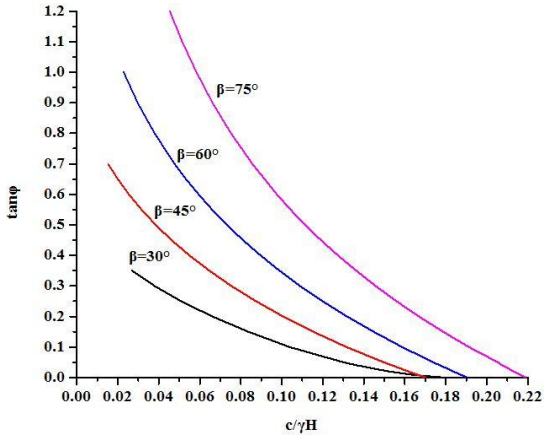

(a) H = 1.5 h, D = 2 m

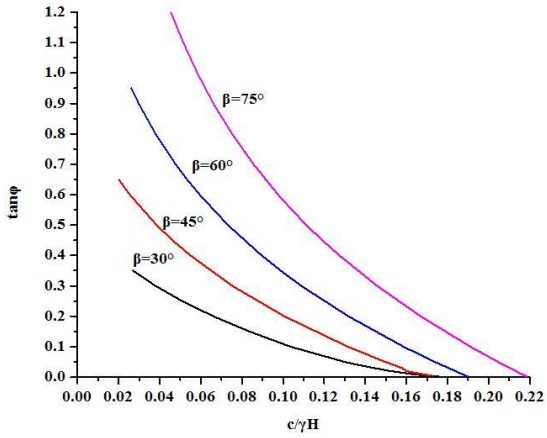

(b) H = 1.5 h, D = 3 m

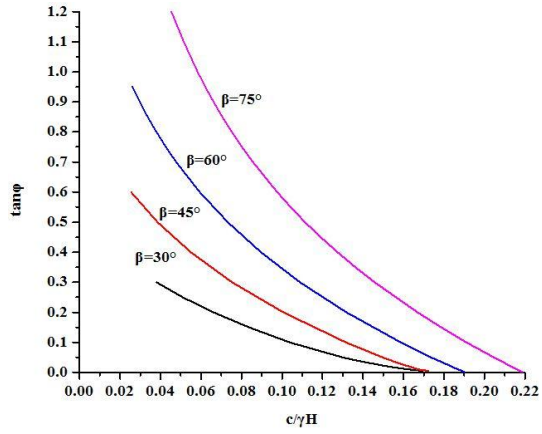

(c) H = 1.5 h, D = 4 m

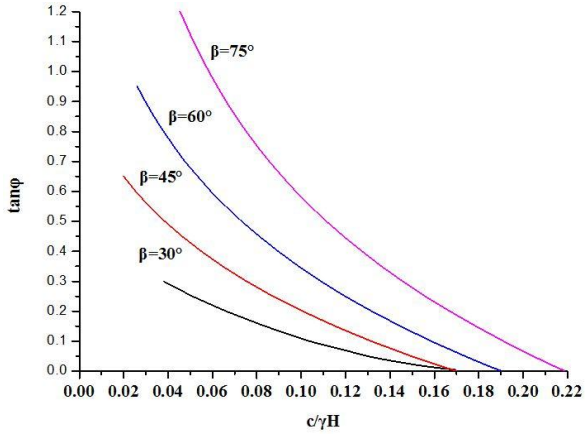

(d) H = 2 h, D = 2 m

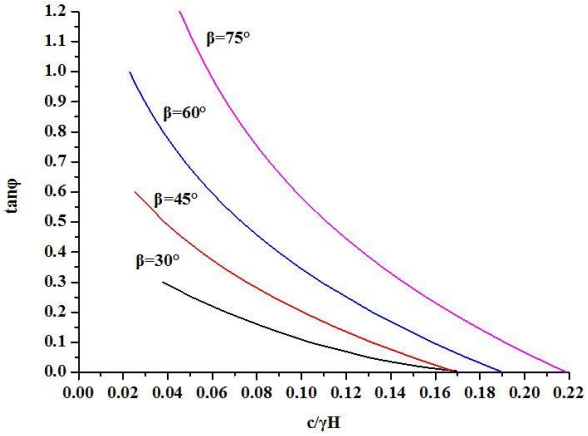

(e) H = 2 h, D = 3 m

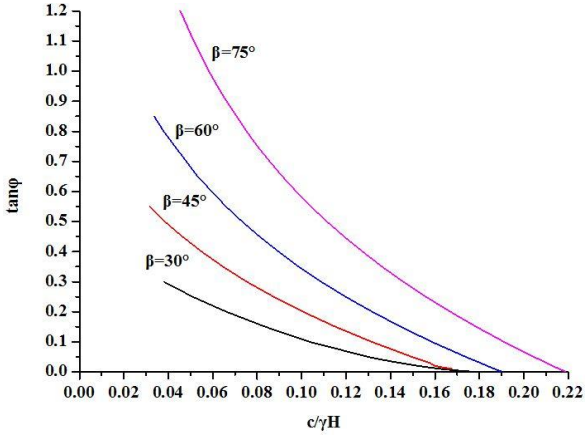

(f) H = 2 h, D = 4 m

Fig. A2 Design charts for slopes with two benches under the simple condition

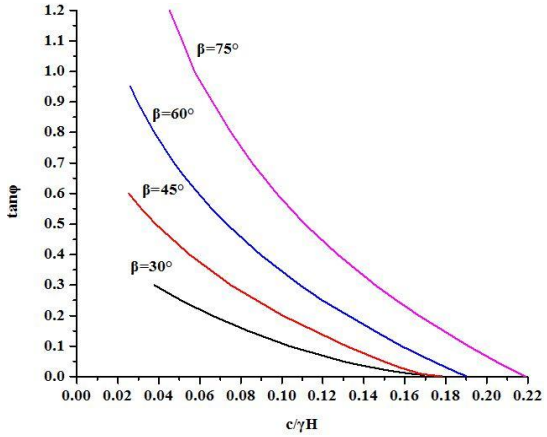

(a) H = 2.5 h, D = 2 m

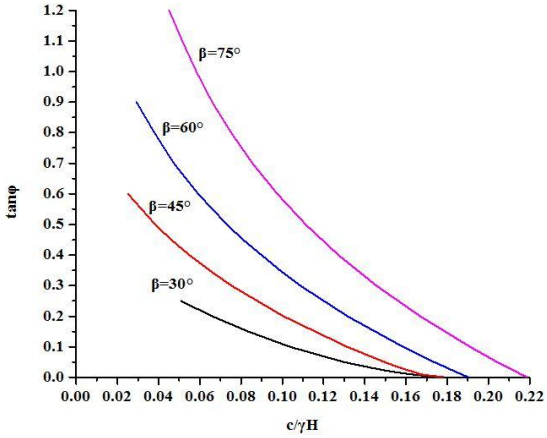

(b) H = 2.5 h, D = 3 m

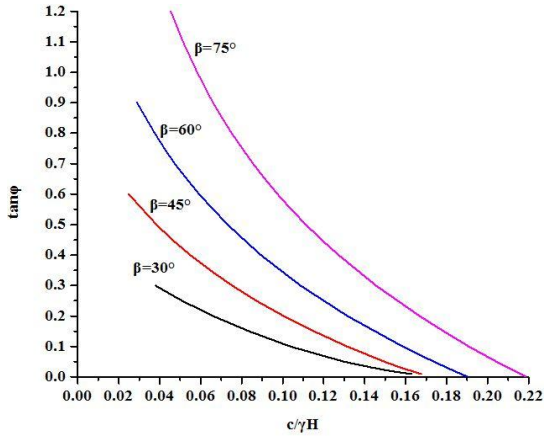

(c) H = 2.5 h, D = 4 m

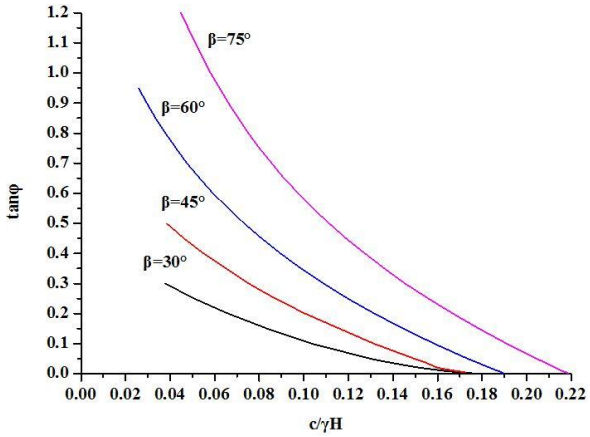

(d) H = 3 h, D = 2 m

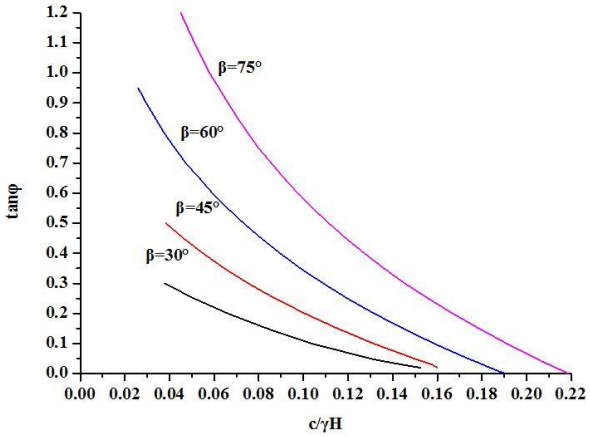

(e) H = 3 h, D = 3 m

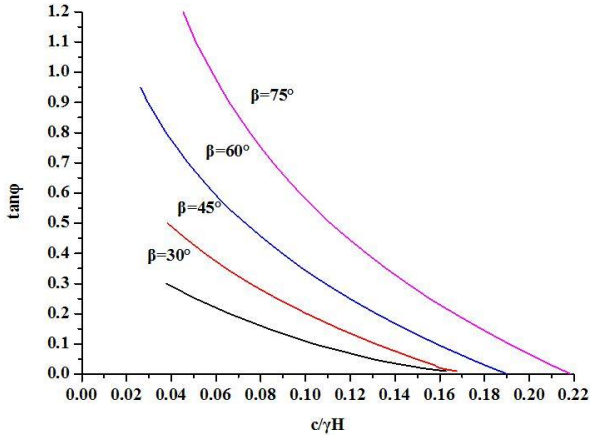

(f) H = 3 h, D = 4 m

Fig. A3 Design charts for slopes with three benches under the simple condition

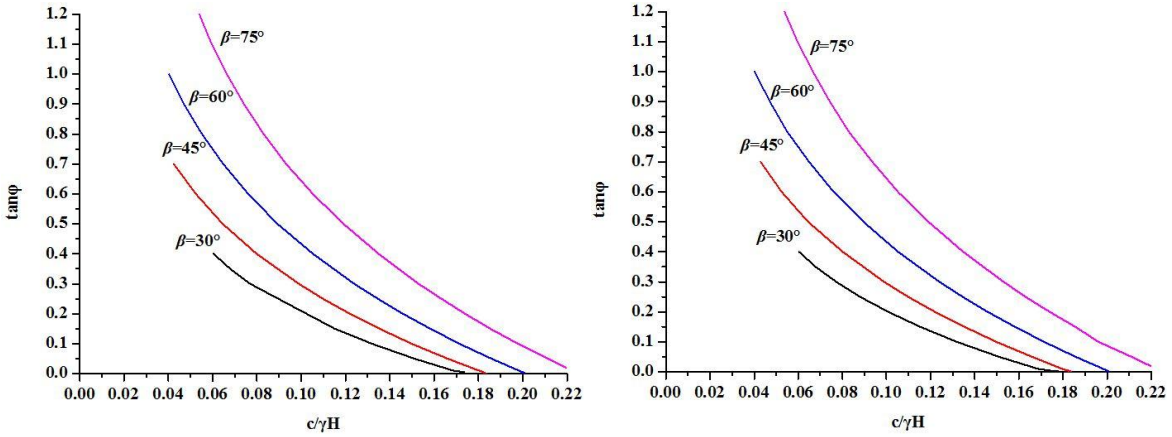

(a) H = 4.5 h, D = 2 m (b) H = 4.5 h, D = 3 m

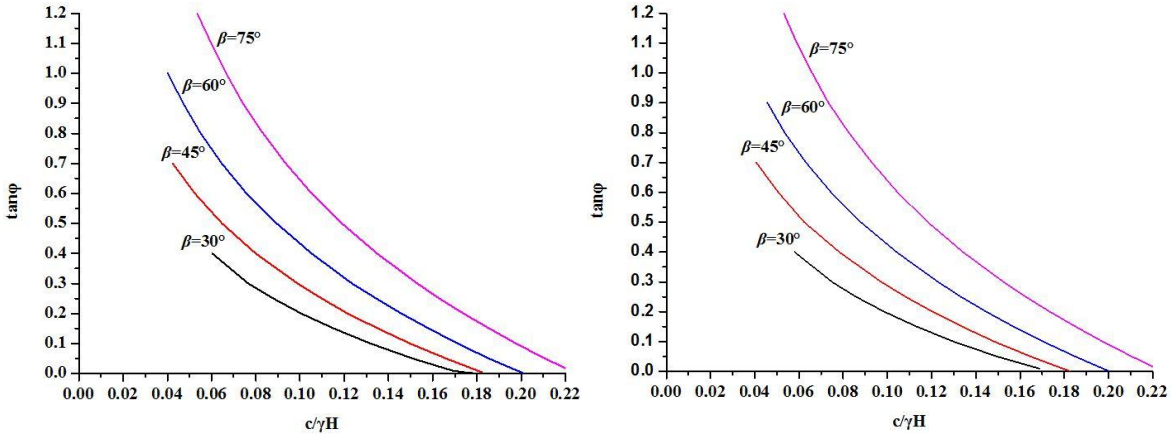

(c) H = 4.5 h, D = 4 m (d) H = 5 h, D = 2 m

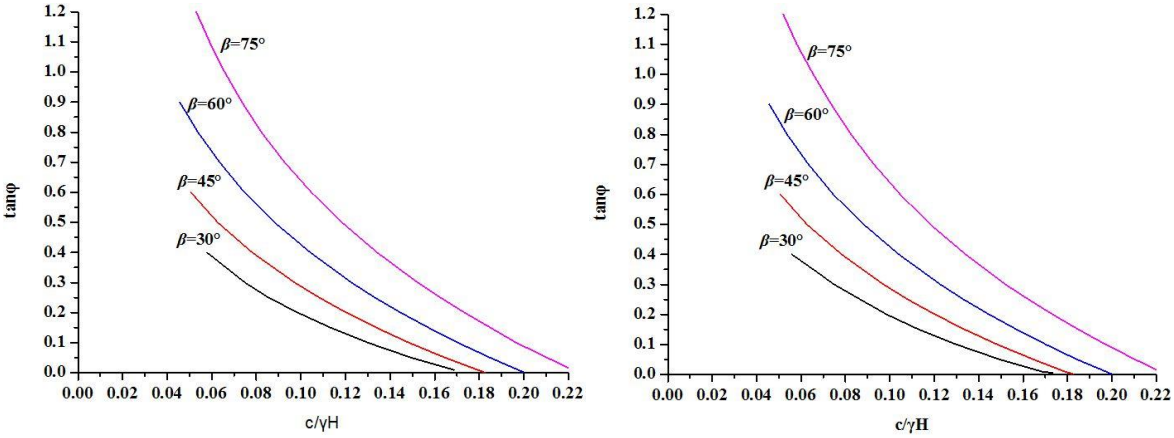

(e) H = 5 h, D = 3 m (f) H = 5 h, D = 4 m

Fig. A4 Design charts for slopes with five benches under the simple condition